

## Carbon Nanotubes

DOI: 10.1002/ange.200601718

**Preparation, Purification, Characterization, and Cytotoxicity Assessment of Water-Soluble, Transition-Metal-Free Carbon Nanotube Aggregates\*\****Hiroyuki Isobe,\* Takatsugu Tanaka, Rui Maeda, Eisei Noiri, Niclas Solin, Masako Yudasaka, Sumio Iijima, and Eiichi Nakamura\**

Besides attracting the attention of scientists and engineers because of potential applications, carbon nanotubes (NTs)

[\*] Dr. H. Isobe, T. Tanaka, R. Maeda, Dr. N. Solin, Prof. E. Nakamura  
Department of Chemistry and  
Center for NanoBio Integration  
The University of Tokyo  
Hongo, Bunkyo-ku, Tokyo 113-0033 (Japan)  
Fax: (+81) 3-5800-6889  
E-mail: hisobe@chem.s.u-tokyo.ac.jp  
nakamura@chem.s.u-tokyo.ac.jp

Dr. E. Noiri  
University Hospital and Center for NanoBio Integration  
The University of Tokyo  
Hongo, Bunkyo-ku, Tokyo 113-0033 (Japan)

Dr. M. Yudasaka, Prof. S. Iijima  
SORST, JST, NEC Corporation  
Tsukuba, Ibaraki 305-8501 (Japan)

Dr. H. Isobe  
PRESTO, JST (Japan)

Prof. E. Nakamura  
ERATO, JST (Japan)

Prof. S. Iijima  
Department of Material Science and Engineering  
Meijo University  
Shiogamaguchi, Tenpaku, Nagoya, Aichi 468-8502 (Japan)

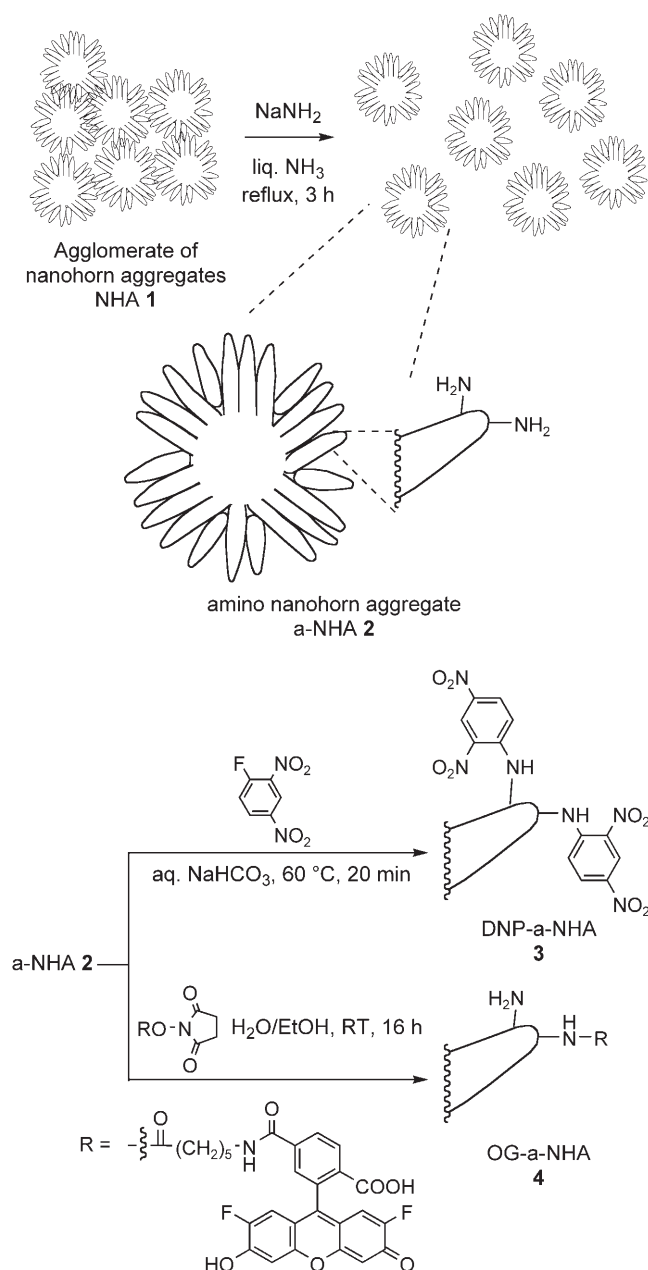
[\*\*] This study was supported in part by Monbukagakusho, Japan (the 21st Century COE Program for Frontiers in Fundamental Chemistry to E.N., grant-in-aid for Scientific Research, Young Scientists (A) to H.I.). We thank Dr. K. Suenaga and Dr. Z. Liu for TEM analysis, Prof. Y. Umezawa and Dr. M. Sato for advice on confocal microscopy, and Dr. J. Miyawaki for Raman spectroscopic measurements. N.S. thanks the Knut och Alice Wallenbergs Stiftelse (Stockholm, Sweden) for a postdoctoral fellowship.

Supporting information for this article is available on the WWW under <http://www.angewandte.org> or from the author.

are also a subject of concern owing to potential medical and environmental problems.<sup>[1–5]</sup> As the NTs belong to a class of graphite that is not toxic, the concern resides mainly in the effect of their nanometer dimensions and the tubular structure with curved surface and fullerene-like end caps. There have been conflicting reports on the biological effects of NTs, some reporting high<sup>[6–11]</sup> and others low toxicity.<sup>[12–14]</sup> Among the issues that complicate the matter are the catalyst metal contaminants in NTs, which have so far been impossible to remove entirely without destroying the structural entity of NTs. A recent report on the genetic response to NTs indicates that risk assessment studies of NTs to date may be viewed as a sum of the effects of NTs and the transition metals,<sup>[15]</sup> some of which are known to be toxic by themselves.<sup>[1]</sup> Another issue is the lack of methods to prepare water-soluble NT particles that are homogeneous enough to ensure validity of the studies on the alleged nanosize effects. The uncontrollable aggregation behavior of NTs, for instance, bundle formation, poses an additional problem that hampers risk assessment studies.<sup>[4,5]</sup> Note that the surfactants used widely for solubilization of NTs<sup>[16,17]</sup> are toxic by themselves and must therefore be avoided. We report here the preparation of a homogenous aqueous solution of approximately 130-nm-sized structurally stable aggregates of entirely metal-free single-walled (SW) NTs, the evidence of persistent uptake into the cytoplasm of mammalian cells, and the low-level cytotoxicity of these particles. In the present study, physicochemical properties of NT samples—size distribution, agglomeration state, shape, chemical composition, surface area, surface chemistry, surface charge, and porosity<sup>[18]</sup>—have been characterized for the first time, and the samples conform to the criteria<sup>[4,5]</sup> specified for nanomaterials samples suitable for toxicological studies. During the studies, we found that NTs disturb the colorimetric bioassays that have been used for risk assessment tests and hence may have affected the reported toxicities of NT materials.

The carbon nanohorn aggregate<sup>[19]</sup> (NHA; Scheme 1) is unique among the NT varieties, and its properties make it suitable for risk assessment studies. First, it has all of the properties of NTs except the high aspect ratio of a single isolated NT. Second, since NHA is a covalently bonded class of self-aggregated NTs, its local peripheral morphology represents the terminal region of a single NT, and the global morphology represents spherically assembled NT bundles (see Figure 1 f and Supporting Information). For instance, its bulk morphology resembles a spherical aggregate of metal-containing NTs previously studied for biological assay.<sup>[10]</sup> Third and most importantly, as NHAs are prepared by laser ablation of a carbon rod without using a transition-metal catalyst, they do not contain any metallic impurities. The NHA as it is prepared forms agglomerates (Scheme 1; cf. Figure 1 c) that cannot be separated physically, and hence they are essentially insoluble in water.

In the first step of our study, we devised a simple and effective method to convert the agglomerates into a water-soluble amino NHAs (a-NHA **2** and its derivatives **3** and **4**) (Scheme 1), which, if necessary, can be chromatographically fractionated according to their size. The approximate molecular weight of these particles as well as the number of the



**Scheme 1.** Chemical transformation of NHA agglomerates into single-particle amino NHA 2 and subsequent derivatization.

amino groups attached to them has been determined (see below). We found that, upon treatment with  $\text{NaNH}_2$ , the NHA agglomerates can be converted, in their entirety, into water-soluble a-NHA 2 (Scheme 1). Treatment of 1.00 g of NHA with  $\text{NaNH}_2$  in refluxing liquid  $\text{NH}_3$  ( $-33^\circ\text{C}$ ) for 3 h, followed by evaporative removal of  $\text{NH}_3$  and washing with aq.  $\text{NH}_4\text{Cl}$  afforded 1.03 g of a-NHA 2 as a black powder. Though the reaction did not cause any obvious change of the powder behavior, the material was now soluble in water. Dilution of 2 in ultrapure water with sonication resulted in a homogeneous black solution with a concentration of up to  $1\text{ mg mL}^{-1}$ . This method for solubilization features low-temperature and basic conditions in contrast to the previously reported methods that

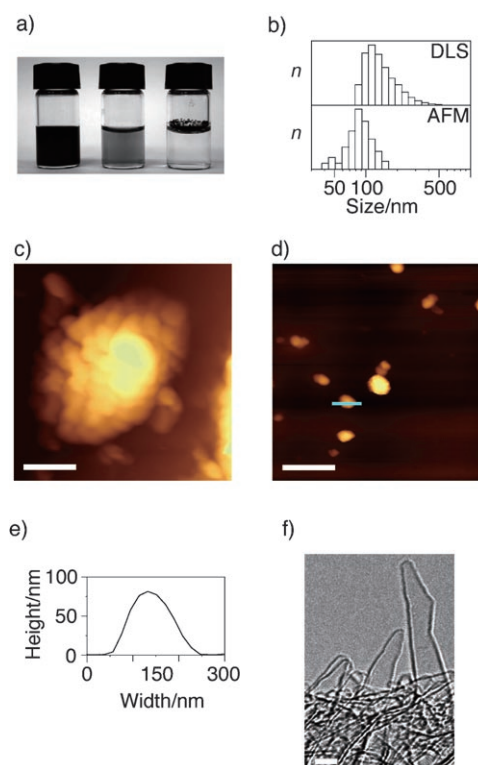


**Figure 1.** Carbon nanohorn aggregate. a) Photographs of solutions of a-NHA 2 in water at concentrations of  $1\text{ mg mL}^{-1}$  (left) and  $0.02\text{ mg mL}^{-1}$  (center) and intact NHA (right). b) Size distribution of 2 in water ( $0.2\text{ mg mL}^{-1}$ ) determined by DLS analysis (top) and of a solution of 2 deposited on mica determined by AFM analysis (bottom). The AFM data was obtained by the height analysis of 117 particles in four images. An average dimensional aspect ratio of the particles was measured to be 2.5:1. c) An AFM image of agglomerate of NHA 1 deposited on HOPG. The outline of single NHA particles in the agglomerate can be seen. Scale bar: 500 nm. d) An AFM image of 2 deposited on mica. Scale bar: 500 nm. e) The height profile of an a-NHA particle measured along the blue line in Figure 1 d. f) TEM image of a-NHA 2 showing that no damage was caused by the  $\text{NaNH}_2$  treatment. Scale bar: 2 nm.

generally rely on oxidation with nitric acid or hot oxygen gas. Note that liquid  $\text{NH}_3$  and  $\text{NaNH}_2$  can be readily removed at room temperature by evaporation and washing with water.

The bulk properties of the aqueous solution of 2 were characterized by dynamic laser light scattering (DLS), atomic force microscopy (AFM), and  $\zeta$  potential measurement. Figure 1a shows homogeneous solutions of 2 with concentrations of  $1\text{ mg mL}^{-1}$  and  $0.02\text{ mg mL}^{-1}$ , which leave no insoluble materials upon filtration through a  $5\text{-}\mu\text{m}$ -pore membrane filter. The vial on the right contains a suspension of the insoluble NHA agglomerate at a concentration of  $0.2\text{ mg mL}^{-1}$ . DLS analysis of more dilute solution of 2 ( $0.2\text{ mg mL}^{-1}$ ; Figure 1b) indicates that the solution contains isolated particles of  $134 \pm 5\text{ nm}$  (average diameter). The size distribution was found to be stable for several months, and the particles did not show any sign of reagglomeration.

AFM analysis of the solution deposited on mica surface showed spheroidal particles distributed on the surface as in Figure 1d. The morphology is entirely different from that of

the NHA agglomerate (Figure 1c). The particles have an average height of 95 nm and an aspect ratio of 2.5:1 (Figure 1d). Such particles would be measured as 122–156 nm by DLS,<sup>[20]</sup> which agrees with the average DLS value of 134 nm. The data also agree with the size estimated previously by transmission electron microscopy (TEM).<sup>[19]</sup> The average particle size (based on AFM) corresponds to an approximate volume of  $1\text{--}3 \times 10^{-21} \text{ m}^3$ . This value coupled with the reported density of  $1.25 \text{ g mL}^{-1}$ <sup>[18]</sup> leads to an estimated molecular weight of  $8\text{--}20 \times 10^8 \text{ Da}$ , which in turn results in an estimate of  $3\text{--}7 \times 10^{11}$  particles per mL in a solution of **2** with a concentration of  $1 \text{ mg mL}^{-1}$ . The  $\zeta$  potential of **2** in ultrapure water was found to be  $-28 \text{ mV}$ . Such negative potentials have been commonly found for carbonaceous materials such as SWNTs and carbon black.<sup>[13,21]</sup>

a-NHA **2** can be separated into fractions according to particle size. After chromatographic purification of the solution ( $0.2 \text{ mg mL}^{-1}$ ) on a polyacrylamide size-exclusion column 92% of the material was recovered (see the chromatogram in Figure 2a). As evident in the DLS data

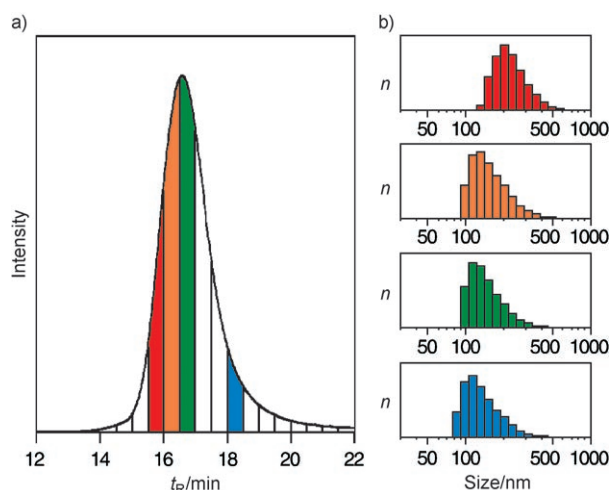


**Figure 2.** Fractionation of a-NHA **2** by gel permeation column chromatography. a) Chromatogram of **2** ( $0.2 \text{ mg mL}^{-1}$ ,  $0.5 \text{ mL}$ ) eluted on Sephacryl 500HR (bed volume:  $17 \text{ mL}$ , detection:  $260 \text{ nm}$ ). Fractions collected at  $t_R = 15.5 \text{ min}$  (red);  $t_R = 16.0 \text{ min}$  (orange);  $t_R = 16.5 \text{ min}$  (green);  $t_R = 18.0 \text{ min}$  (blue). b) DLS analysis of the representative fractions. Mean sizes of particles in fractions are  $198 \pm 17$ ,  $148 \pm 1$ ,  $134 \pm 6$  and  $127 \pm 7 \text{ nm}$ , respectively. The color code of the fractions corresponds to the colored fractions in (a).  $t_R$  = time of retention.

measured for four representative fractions (Figure 2b), chromatographic separation of a-NHA of various sizes (127, 134, 148, and 198 nm, mean diameter) has been achieved. We expect that further optimization of the chromatographic conditions will result in better resolution.

Chemical characterization of the water-soluble NHA indicated that  $\text{NaNH}_2$  treatment has introduced amino groups on the surface of the graphitic structure. Careful TEM observation (Figure 1f and Supporting Information) showed that there has been no change of the gross SWNT structure; that is, neither holes nor added materials were

observed. The UV/Vis spectra of **2** in water show a broad absorbance due to the tubular graphite (Supporting Information). Thermal gravimetric analysis (TGA) and Raman spectra suggest that the amination reaction under mild conditions did not cause any significant change of the gross NHA structure.<sup>[22,23]</sup> The presence and the quantity of the amino groups on **2** were determined by the Sanger method used widely for characterization of amino groups in proteins.<sup>[24]</sup> Treatment of **2** with 4-fluoro-1,3-dinitrobenzene (Scheme 1) gave a water-soluble black powder that exhibits an absorption at  $350 \text{ nm}$  (Supporting Information). This is characteristic of the dinitrophenylamino (DNP) group and is not observed for the two starting materials. Neither excess reagent nor longer reaction time led to an increase of the  $350\text{-nm}$  absorption, and we conclude that all available amino groups have been dinitrophenylated.

On the basis of the known molar absorption coefficient of the DNP group and the value measured for DNP-a-NHA (**3**), we calculate the amount of the amino group to be  $0.22 \mu\text{mol mg}^{-1}$ . A density of one amino group per 380 carbon atoms can be thus calculated. It is reasonable to assume that the amination reaction took place on the exposed surface, which can be estimated from the surface area available for  $\text{N}_2$  absorption. The reported surface area of NHA,  $308 \text{ m}^2 \text{ g}^{-1}$ ,<sup>[18]</sup> and the calculated amine density gives an estimated amine density on the surface to be one amino group per 46 carbon atoms. This ratio suggests that the reaction occurred on the reactive cap or bent regions rather than on the smooth surface of the tube.

Similarly, we introduced fluorescent Oregon Green (OG) dye to the a-NHA. To maintain water-solubility, we exposed the fluorescent probe to only 8% of the available amino groups. The presence and the amount of the probe were determined by quantitative absorption and fluorescence spectroscopic analysis (Supporting Information).

With the physicochemical data of the soluble NHAs in hand, we investigated the cell uptake and the toxicity of this material. The soluble labeled OG-a-NHA **4** (Scheme 1, used as such without fractionation of particles) was incubated with growing mammalian cells (3T3 and HeLa cells), and the cell uptake was monitored by flow cytometry (FCM). As shown in Figure 3, the amount of **4** in the cells showed dose- ( $0.01 \text{ mg mL}^{-1}$  vs.  $0.05 \text{ mg mL}^{-1}$ ) and time-dependent increase.<sup>[12,13,25]</sup> Notably, the uptake per cell increased persistently for 22 h.

The location of OG-a-NHA **4** in the cells after an incubation time of 20 h was determined by microscopy (Figure 3c and d). The black spots several  $\mu\text{m}$  in size seen in Figure 3c are agglomerates of **4** located within the cytoplasm.<sup>[26]</sup> Smaller particles of **4** are seen as green fluorescent particles in Figure 3d. The cell membrane stained by FM4-64 appears red in Figure 3d, and the yellowish area represents the overlap of the red and green colors, thus indicating that **4** is not located in the outer cell membrane but within the cytoplasm.

Having learned that a-NHA readily enters into mammalian cells, we next examined its cytotoxicity. We used quartz particles of  $5 \mu\text{m}$  in size and  $\text{TiO}_2$  particles of  $25\text{--}70 \text{ nm}$  in size (primarily anatase) as controls.<sup>[4]</sup> While both are used widely



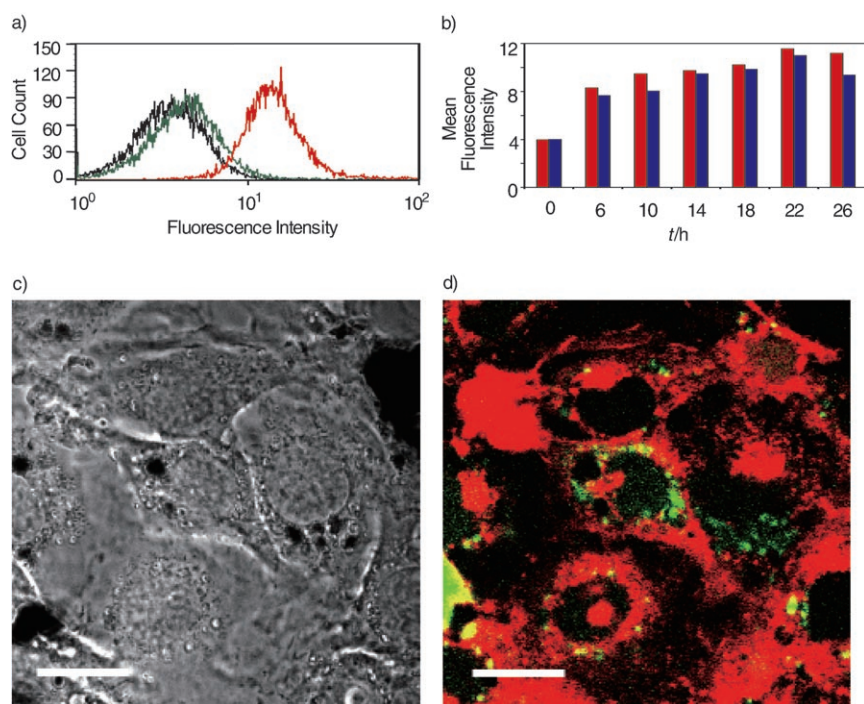


**Figure 3.** FCM and confocal microscopic analysis of OG-a-NHA **4** taken up by cultured mammalian cells. a) Fluorescence histograms of control cells (black; 3T3 cells) and cells incubated with **4** at concentrations of 0.01 mg mL<sup>-1</sup> (green) and 0.05 mg mL<sup>-1</sup> (red). b) Time-dependent fluorescent intensity of cells (3T3: red; HeLa: blue) incubated with **4** (0.05 mg mL<sup>-1</sup>). c) Phase contrast image of 3T3 cells after incubation with **4** (0.05 mg mL<sup>-1</sup>) for 20 h. Scale bar: 20 μm. d) Confocal microscope image of the same region as in (c). OG-a-NHA **4** was observed with the fluorescence at 518 nm (green), and the cell membrane was stained with FM4-64 and observed with the fluorescence at 590 nm (red).

in industry, the former shows a certain level of cytotoxicity<sup>[7,8]</sup> and the latter is considered nontoxic. We examined the cytotoxicity for two standard cell lines (3T3 and HeLa cells) by using quantitative Bradford protein assay,<sup>[27]</sup> where the protein is freed of the carbon material at the time of analysis (vide infra). In the quartz control experiments for 3T3 cells, 0.1 mg mL<sup>-1</sup> of the quartz powder dropped the cell activity to 75 % and 1 mg mL<sup>-1</sup> to 28 %, but TiO<sub>2</sub> showed no cytotoxicity up to 1 mg mL<sup>-1</sup>. As shown in Figure 4, a-NHA **2** shows no cytotoxicity up to 0.1 mg mL<sup>-1</sup>, but at the 1.0-mg dose the cell activity dropped to 78 % (3T3) and 74 % (HeLa). The cytotoxicity of the a-NHA is therefore one-tenth of that of quartz microparticles by weight.

In conclusion, aminative deagglomeration of NHA agglomerates resulted, for the first time, in the high-yielding preparation of well-characterized NHA, which form homogeneous aqueous solutions of primary particles of uniform size distribution. Unlike the NT materials synthesized under transition-metal catalysis, our samples do not contain any transition-metal impurities. The preparative method is very simple and amenable to large-scale syntheses. The primary particles thus obtained could not be disintegrated further into individual NTs either physically or chemically. Therefore, the amino NHA particle may be regarded as a big macromolecule. The amination method and subsequent chromatographic purification provide transition-metal-free SWNT materials that are available in a variety of sizes ranging from 80 nm to

400 nm; these materials may thus serve as standards for risk assessment of carbon nanoparticles. In a sense, the amino NHA is a congener of water-soluble fullerenes, whose biological activities have been studied since the early 1990s.<sup>[28–34]</sup>

As expected for water-soluble materials 100 nm in size,<sup>[35]</sup> the amino NHA is taken up by mammalian cells but does not show significant cytotoxicity; in fact, the cytotoxicity is much lower than that of the quartz microparticles widely used in road-marking paints. Nonetheless, appropriate care must be taken in handling since it would be persistently taken up by growing cells. We argue that the observed level of cytotoxicity may possibly arise from the removal of necessary nutrients by absorption on the surface (see below), chemical effects of the amino groups attached to the NHA surface, or certain profound effects of the nanographitic structure on the crucial mechanism of life. The low toxicity described above stands in contrast to some reports reporting that NTs are much more toxic than quartz microparticles.<sup>[8–10]</sup> In addition to the problem of the metal impurities discussed above,

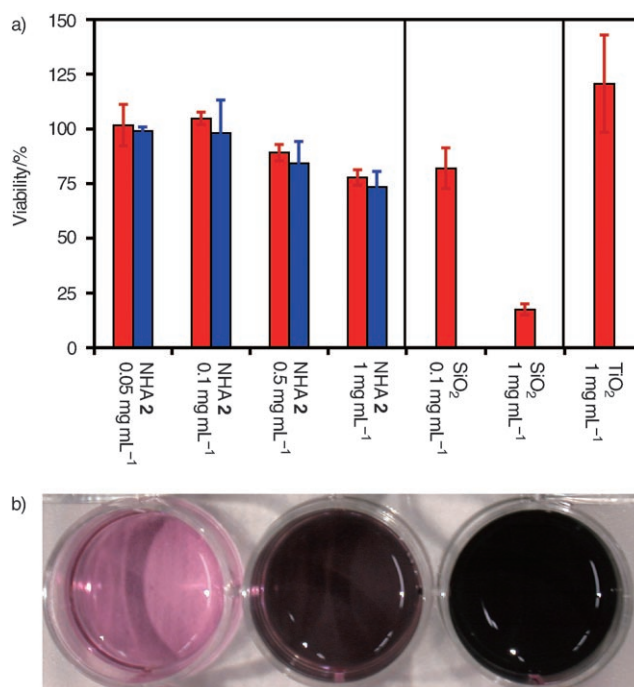


**Figure 4.** Cytotoxicity assessment of a-NHA. a) Viability of 3T3 (red) and HeLa (blue) cells after incubation with particles for 24 h. Viability was determined by the Bradford assay. b) Photograph of culture dish of 3T3 cells. Control (left, pink color due to phenol red pH indicator) and in the presence of a-NHA **2** at the concentrations of 0.1 mg mL<sup>-1</sup> (center) and 1 mg mL<sup>-1</sup> (right).

another caveat of the bioassays of NT-like compounds that we discovered in the present study is that such graphitic materials reduce the coloration of the aromatic dye employed in the assay and hence result in false data. Thus, dye-based assays of cell viability such as the MTT (3-(4,5-dimethylthiazol-2-yl)-2,5-diphenyltetrazolium bromide) assay, the Alamar Blue test, and the propidium iodide test, which have been used in the NT bioassays, uniformly gave us incorrect results unless care was taken to prevent contact of the graphitic materials with the dye (details in the Supporting Information).

Received: May 2, 2006

Revised: July 27, 2006

**Keywords:** amination · cellular uptake · liquid chromatography · nanotubes · toxicology

- [1] V. L. Colvin, *Nat. Biotechnol.* **2003**, *21*, 1166–1170.
- [2] R. F. Service, *Science* **2004**, *304*, 1732–1734.
- [3] R. F. Service, *Science* **2005**, *310*, 1609.
- [4] G. Oberdörster, A. Maynard, K. Donaldson, V. Castranova, J. Fitzpatrick, K. Ausman, J. Carter, B. Karn, W. Kreyling, D. Lai, S. Olin, N. Monteiro-Riviere, D. Warheit, H. Yang, *Part. Fibre Toxicol.* **2005**, *2*, (<http://www.particleandfibretoxicology.com/content/2/1/8/>).
- [5] R. H. Hurt, M. Monthieux, A. Kane, *Carbon* **2006**, *44*, 1028–1033.
- [6] D. B. Warheit, B. R. Laurence, K. L. Reed, D. H. Roach, G. A. M. Reynolds, T. R. Webb, *Toxicol. Sci.* **2004**, *47*, 117–125.
- [7] C.-W. Lam, J. T. James, R. McCluskey, R. L. Hunter, *Toxicol. Sci.* **2004**, *47*, 126–134.
- [8] G. Jia, H. Wang, L. Yan, X. Wang, R. Pei, T. Yan, Y. Zhao, X. Guo, *Environ. Sci. Technol.* **2005**, *39*, 1378–1383.
- [9] L. E. Murr, K. M. Garza, K. F. Soto, A. Carrasco, T. G. Powell, D. A. Ramires, P. A. Guerrero, D. A. Lopez, J. Venzor III, *Int. J. Environ. Res. Public Health* **2005**, *2*, 31–42.
- [10] K. F. Soto, A. Carroscio, T. G. Powell, K. M. Garza, L. E. Murr, *J. Nanopart. Res.* **2005**, *7*, 145–169.
- [11] S. K. Manna, S. Sarkar, J. Barr, K. Wise, E. V. Berrera, O. Jejelowo, A. C. Rice-Ficht, G. T. Ramesh, *Nano Lett.* **2005**, *5*, 1676–1684.
- [12] D. Pantarotto, J.-P. Briand, M. Prato, A. Bianco, *Chem. Commun.* **2004**, 16–17.
- [13] N. W. S. Kam, T. P. Jessop, P. A. Wender, H. Dai, *J. Am. Chem. Soc.* **2004**, *126*, 6850–6851.
- [14] T. Murakami, K. Ajima, J. Miyawaki, M. Yudasaka, S. Iijima, K. Shiba, *Mol. Pharm.* **2004**, *1*, 399–405.
- [15] L. Ding, J. Stilwell, T. Zhang, O. Elboudwarej, H. Jiang, J. P. Selegue, P. A. Kooke, J. W. Gray, F. F. Chen, *Nano Lett.* **2005**, *5*, 2448–2464.
- [16] M. J. O'Connell, S. M. Bachilo, C. B. Huffman, V. C. Moore, M. S. Strano, E. H. Haroz, K. L. Rialon, P. J. Boul, W. H. Noon, C. Kittrell, J. Ma, R. H. Hauge, R. B. Weisman, R. E. Smalley, *Science* **2002**, *297*, 593–596.
- [17] M. Zhang, M. Yudasaka, J. Miyawaki, J. Fan, S. Iijima, *J. Phys. Chem. B* **2005**, *109*, 22201–22204.
- [18] K. Murata, K. Kaneko, F. Kokai, K. Takahashi, M. Yudasaka, S. Iijima, *Chem. Phys. Lett.* **2000**, *331*, 14–20.
- [19] S. Iijima, M. Yudasaka, R. Yamada, S. Bandow, K. Suenaga, F. Kokai, K. Takahashi, *Chem. Phys. Lett.* **1999**, *309*, 165–170.
- [20] W. Van De Sande, A. J. Persoons, *Phys. Chem.* **1985**, *89*, 404–406.
- [21] R. Xu, *Particle Characterization: Light Scattering Methods*, Kluwer, Dordrecht, Netherlands, **2000**, pp. 289–343.
- [22] Weight loss of **2** occurred at 560°C in TGA, which is slightly lower than that observed for the intact NHA (J. Miyawaki, M. Yudasaka, S. Iijima, *J. Phys. Chem. B* **2004**, *108*, 10732–10735).
- [23] The intensity ratio of the G-band (1590 cm<sup>-1</sup>) and the D-band (1350 cm<sup>-1</sup>) in Raman spectra of **2** and intact NHA were 0.96 and 0.91, respectively.
- [24] C. H. W. Hirs, *Methods Enzymol.* **1967**, *11*, 548–555.
- [25] N. W. S. Kam, Z. Liu, H. Dai, *Angew. Chem.* **2006**, *118*, 591–595; *Angew. Chem. Int. Ed.* **2006**, *45*, 577–581.
- [26] Since the larger particles of the NHA scatter light and are seen as black in the image, the actual amount of **4** in cells would be greater than that determined with FCM.
- [27] M. M. Bradford, *Anal. Biochem.* **1976**, *72*, 248–254.
- [28] S. H. Friedman, D. L. DeCamp, R. P. Sijbesma, G. Srdanov, F. Wudl, G. L. Kenyon, *J. Am. Chem. Soc.* **1993**, *115*, 6506–6509.
- [29] R. F. Schinazi, R. Sijbesma, G. Srdanov, C. L. Hill, F. Wudl, *Antimicrob. Agents Chemother.* **1993**, *37*, 1707–1710.
- [30] H. Tokuyama, S. Yamago, E. Nakamura, T. Shiraki, Y. Sugiura, *J. Am. Chem. Soc.* **1993**, *115*, 7918–7919.
- [31] S. Yamago, H. Tokuyama, E. Nakamura, K. Kikuchi, S. Kananishi, K. Sueki, H. Nakahara, S. Enomoto, F. Ambe, *Chem. Biol.* **1995**, *2*, 385–389.
- [32] E. Nakamura, H. Isobe, N. Tomita, M. Sawamura, S. Jinno, H. Okayama, *Angew. Chem.* **2000**, *112*, 4424–4427; *Angew. Chem. Int. Ed.* **2000**, *39*, 4254–4257.
- [33] S. Bosi, T. Da Ros, G. Spalluto, M. Prato, *Eur. J. Med. Chem.* **2003**, *38*, 913–923.
- [34] E. Nakamura, H. Isobe, *Acc. Chem. Res.* **2003**, *36*, 807–815.
- [35] H. Isobe, W. Nakanishi, N. Tomita, S. Jinno, H. Okayama, E. Nakamura, *Chem. Asian J.* **2006**, *1*, 167–175.
- [36] H. Gao, W. Shi, L. B. Freund, *Proc. Natl. Acad. Sci. USA* **2005**, *102*, 9469–9474.